Contrib Mineral Petrol (1982) 79: 187–200

Contributions to Mineralogy and Petrology

Crystal Growth and the Formation of Chemical Zoning in Garnets

Randall T. Cygan and Antonio C. Lasaga
Department of Geosciences, The Pennsylvania State University, University Park, Pennsylvania 16802, USA

Abstract. A crystal growth model is developed which generalizes the Rayleigh fractionation process. The new growth model allows some insight into the interpretation of nonequilibrium behavior of minerals, primarily the chemical zoning profiles exhibited by metamorphic minerals. A nonlinear equilibrium term for exchange of constituents between a growing mineral and a reservoir is initially incorporated into the usual isothermal fractionation model. Criteria are established to decide when a simple distribution term is sufficient to describe the growth and exchange process. The model is then extended to allow for temperature changes during a cooling or heating event. Finally, an exact solution is obtained for the temperature dependent case incorporating a time dependent growth rate. The growth models are successfully used to obtain growth rates of 0.01 to 0.09 cm/million year and describe the magnesium and iron zoning profiles of garnets from Phillipston, Massachusetts. The generalized model confirms the development of zoning during the retrograde growth of garnet in the late stages of the Acadian orogeny.

Introduction

Compositional zoning of silicate minerals has been recognized as a common feature in numerous geological environments. This disequilibrium feature is most frequently observed in metamorphic garnets where the relatively slow diffusion kinetics prevent complete chemical homogenization across the grain. Qualitative descriptions of the formation of this chemical zoning are common features in the geologic literature (Atherton and Edmunds 1966; Harte and Henley 1966; Linthout and Westra 1968; Blackburn 1969; Brown 1969; Emiliani and Venturelli 1972; de Béthune et al. 1975; Woodsworth 1977; Yardley 1977; Finlay and Kerr 1979). Only recently has there been an attempt to quantify the generation of compositional zoning patterns.

Three general models are normally relied upon to explain the zoning patterns of natural garnets: (1) An isothermal fractionation model where an element is isothermally partitioned and isolated into a growing garnet from a homogeneous reservoir which, in turn, is being depleted in that element (Hollister 1966; Atherton 1968, 1976; Miyashiro and Shido 1973); (2) Chemical diffusion and exchange during and after crystal growth producing concentration gradients in the garnet and/or the neighboring phase as especially developed by Lasaga et al. (1977) (see also Anderson and Buckley 1973, 1974; Loomis 1975); (3) Growth during prograde (or retrograde) metamorphism where the changing temperatures appropriately alter the equilibrium distribution terms during the garnet crystallization (Grant and Weiblen 1971; Miyashiro and Shido 1973; Tracy et al. 1976). All of these models, separately or combined, have been successful in generating compositional profiles which approximate those observed in some metapelitic garnets.

In this paper we develop an important extension of the existing models which allows for crystal growth as temperature and pressure conditions, as well as the bulk composition, change with time. A significant modification is the incorporation of a temperature dependent, and therefore time dependent, fractionation factor for a prograde or retrograde metamorphic reaction. This model would therefore overcome the difficulty of explaining the complex behavior of certain zoning patterns normally ascribed to temperature fluctuations in the *isothermal* fractionation models of Hollister (1966) and Atherton (1968).

In the first section of this paper we discuss the common isothermal fractionation model and some of the difficulties encountered in its application. In the second section we redefine the fractionation factor in its more proper form as a nonlinear equilibrium constant and examine its effect on the predicted zoning profiles. In the third section, we expand the fractionation model to include changing temperature conditions and constant growth velocities. The theory is applied in section four to natural almandine-pyrope garnets from the Phillipston area of Massachusetts. Finally, in section five we extend our model to include a time dependent growth velocity term. This final refinement successfully predicts the natural garnet profiles in the metamorphic assemblage of central Massachusetts and provides a completely general model for application in other crystal growth problems.

Isothermal Fractionation Model

The isothermal garnet growth and fractionation model is based upon the treatment of distillation originally proposed by Rayleigh (1902) for the condensation of a multicomponent vapor. This growth model, also called the segregation-depletion model, describes the zoning pattern for a garnet which grows from a *homogeneous* reservoir. The following equation, as derived by Hollister (1966), describes the weight fraction of an element in the garnet edge as a function of the amount of garnet crystallized from the rock:

0010-7999/82/0079/0187/$02.80

$$M_G = \lambda M_0 \left(1 - \frac{W^G}{W^0}\right)^{\lambda - 1}. \quad (1)$$

The notation used by Hollister, which will be continued in our subsequent derivations, is given below:

M_G = weight fraction of cation in garnet edge
M_0 = initial weight fraction of cation in reservoir prior to garnet crystallization
M_R = weight fraction of cation in reservoir
W^G = total weight of crystallized garnet
W^0 = initial weight of reservoir required for growth of single garnet
λ = fractionation factor, M_G/M_R.

Equation (1) assumes *local* equilibrium for the exchange of the cation between the garnet edge and the surrounding mineral reservoir. The constituents of the garnet are essentially removed from the system as the garnet continues to grow. This leads to a change in the bulk composition of the reactive system. The reservoir of minerals, on the other hand, will reequilibrate in response to this slight depletion of the cation thereby maintaining homogeneity. The factor λ is assumed constant, and represents the fractionation of a cation between the garnet edge and the reservoir minerals. In applications, this factor is normally obtained from the garnet composition at the center of the grain and the initial composition of the entire assemblage.

Several other assumptions are inherent in the derivation of the model. Little or no diffusion in the crystallizing solid is assumed. Garnet, having one of the smallest cation diffusion coefficients for minerals, is therefore best suited for application of the model. This assumption is more valid at low grade conditions where the thermally activated diffusion process is essentially shut off (see Lasaga et al. 1977). In addition, transport within the mineral reservoir is assumed fast enough so that the cation concentration there is uniform. Atherton (1976) provides a comprehensive discussion of the fractionation model and elaborates on the necessary assumptions and limitations of the model.

Hollister (1966) was able to reproduce the variation in MnO content of several almandine garnets from British Columbia by his fractionation model. Curve a of Fig. 1 represents the compositional profile as predicted by his model. This curve approximates the measured garnet compositional profile as represented by the dots. Deviations between the calculated curve and the measured profile are primarily attributed by Hollister to variations in the fractionation factor during the crystallization process. Temperature change was assumed to be the major source for these variations. Large compositional changes in the particular cation would also vary the fractionation factor (see below). The use of a fractionation factor, λ, in the derivation of the model assumes that the cation behaves as a trace element and therefore may not be appropriate for describing major cation partitioning. Finally, the value of λ could be affected by the changing proportions of ferromagnesian reservoir minerals throughout the growth history of the garnet (see Hollister 1969).

Atherton (1968) applied a similar isothermal fractionation model to describe the MnO zoning patterns of medium grade garnets from Scotland. Several of the profiles required a changing fractionation factor to represent the different stages of crystal growth during the prograde event. Atherton therefore fitted each section of the measured profile separately using a different fractionation factor, λ, for each stage of growth (see Fig. 6 of Atherton 1968).

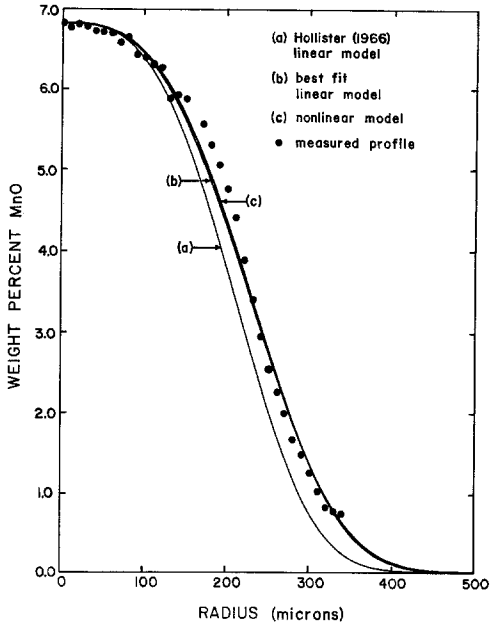

Fig. 1. Theoretical compositional profiles for MnO in garnet: (*a*) Rayleigh fractionation model, $\lambda = 23$, $A = 3619\,\mathrm{cm}^{-3}$; (*b*) improved fit of isothermal fractionation model, $\lambda = 23$, $A = 2624\,\mathrm{cm}^{-3}$; (*c*) corresponding isothermal exchange equilibrium model, $K_D = 24.6$, $a = 1$, $A = 2624\,\mathrm{cm}^{-3}$. The *dots* represent the measured profile of MnO taken from Hollister (1966). (A is defined by Eq. (16))

The simple isothermal fractionation model, although crude, does manage to adequately describe the zoning of certain garnets. Low and medium grade garnets, which have had little or no modification by chemical diffusion, are the likely candidates for the application of this model, especially if they grew within a restricted time span so as to approximate nearly constant temperature conditions. More complicated growth histories (e.g., temperature changes, multiple garnet producing reactions and several stages of growth) restrict the use of this simple model in describing the complex zoning common to most natural garnets. To generalize this fractionation model, it is important to remove the restrictions imposed by the need to maintain constant temperature and the need to ignore major element compositional effects upon the fractionation factor. In the next section we extend the isothermal model to allow for the treatment of major elements by incorporating a nonlinear fractionation term.

Exchange Equilibrium Fractionation Model

The Nernst distribution coefficient is well defined only for a trace element. In this case, we can write:

$$\lambda = \frac{M_G}{M_R} \quad (2)$$

where it will be important in what follows to use weight percent or weight fraction instead of mole fractions. The use of λ will restrict the application of the fractionation model to only the minor or trace cations. With large values of the cation concentration, however, λ becomes compositionally dependent upon the other cations. Using the model to describe major element zoning would require redefining the fractionation factor as an exchange equilibrium constant, K_D:

$$K_D=\frac{M_G M'_R}{M_R M'_G}. \tag{3}$$

M'_G and M'_R are the weight *fractions* of the other major cation undergoing exchange in the garnet and the reservoir, respectively, for a two component system. Equation (3) assumes that mole fractions and weight fractions are directly proportional. Of course, we would ultimately have to deal also with changing activity coefficients.

If $MgAl_{2/3}SiO_4$ and $FeAl_{2/3}SiO_4$ are selected as the components for the garnet, then the sum of the weight fractions is unity, assuming there are no other components (by definition of weight fraction). On the other hand, the reservoir contains several minerals and the weight fractions of $MgAl_{2/3}SiO_4$ and $FeAl_{2/3}SiO_4$ will *not* add up to unity. For example, if the garnet producing reaction is:

$$3\,Mg_2Al_4Si_5O_{18}\rightarrow 2\,Mg_3Al_2Si_3O_{12}+4\,Al_2SiO_5+5\,SiO_2$$
cordierite garnet sillimanite quartz

then the weight fraction of Mg in the reservoir is:

$$M^R_{Mg}=\frac{W_{MgAl_{2/3}SiO_4}}{W_{cord}+W_{sill}+W_{qtz}}$$

where

$$W_{MgAl_{2/3}SiO_4}=\frac{134.4}{292.5}W_{Mg\text{-}cord}.$$

Likewise:

$$M^R_{Fe}=\frac{W_{FeAl_{2/3}SiO_4}}{W_{cord}+W_{sill}+W_{qtz}}$$

where

$$W_{FeAl_{2/3}SiO_4}=\frac{165.9}{324.0}W_{Fe\text{-}cord}.$$

Therefore,

$$M^R_{Mg}+M^R_{Fe}=\frac{0.459\,W_{Mg\text{-}cord}+0.512\,W_{Fe\text{-}cord}}{W_{Mg\text{-}cord}+W_{Fe\text{-}cord}+W_{other\,minerals}}=a<1.$$

It should be noted that to a good approximation the weight fraction of Mg or Fe in garnet will be directly proportional to the mole fraction. In the case of the cordierite breakdown, the weight fraction will also be proportional to the mole fraction in cordierite. (Note that the weight of the other minerals can be minimized, since all minerals not involved in the garnet reaction can be ignored.) The equilibrium expression constant in Eq. (3) can therefore be rewritten:

$$K_D=\frac{M_G(a-M_R)}{M_R(1-M_G)}. \tag{4}$$

A theoretically correct equilibrium constant is usually defined using molar quantities and not the weight fractions required for the present derivation. It can be shown for most cases that this new K_D is essentially independent of composition once the weight fractions have been defined in terms of the mineral end members (e.g., $MgAl_{2/3}SiO_4$ for Mg in garnet). We will be ignoring changes in the activity coefficients assuming ideal mixing in both the garnet and the reservoir *or* by incorporating them into K_D. Note that Eq. (4) reduces to the corresponding linear fractionation term, Eq. (2), as the weight fraction terms approach trace concentration values. In this limit, we find that $K_D=a\lambda$. This last relation is important in what follows.

The initial differential equation for the derivation of the Rayleigh fractionation model is based on mass balance constraints (hence the use of *weight* fractions) between the growing garnet and the mineral reservoir and on the assumption that the garnet is subsequently removed and prevented from back-reacting with the reservoir. We therefore have the following relations among the changes in the contents of the different phases:

$$M_G=\frac{-dW^R_m}{-dW_R}=\frac{dW^G_m}{dW^G}. \tag{5}$$

The additional terms are defined as follows:
W^R_m = weight of cation in reservoir
W_R = weight of reservoir
W^G_m = weight of cation in garnet.
Solving for M_G in Eq. (4), we obtain:

$$M_G=\frac{K_D M_R}{a+M_R(K_D-1)}. \tag{6}$$

Inserting Eq. (6) for M_G into the mass balance equation (Eq. 5) describing the reservoir weight change, we obtain:

$$\frac{dW^R_m}{dW_R}=\frac{K_D M_R}{a+M_R(K_D-1)}. \tag{7}$$

M_R can be written in terms of the absolute weight values as:

$$M_R=\frac{W^R_m}{W_R} \tag{8}$$

which gives the following differential equation with only W^R_m and W_R as variables:

$$\frac{dW^R_m}{dW_R}=\frac{K_D\left(\frac{W^R_m}{W_R}\right)}{a+\left(\frac{W^R_m}{W_R}\right)(K_D-1)}. \tag{9}$$

K_D is constant in the isothermal fractionation model. The solution to this equation, as developed in Appendix A, is given below:

$$\frac{W_R}{W^0}=\left(\frac{M_R-1}{M_0-1}\right)^{\frac{1-K_D-a}{K_D-a}}\left(\frac{M_R}{M_0}\right)^{\frac{a}{K_D-a}}. \tag{10}$$

Equation (8) has been introduced to obtain an expression in terms of the weight fraction of the cation in the reservoir, M_R. To get the final expression in terms of the garnet weight and the cation concentration in the garnet we require two more relationships:

$$W_R=W^0-W^G, \tag{11}$$

$$M_R=\frac{aM_G}{K_D(1-M_G)+M_G}. \tag{12}$$

Equation (11) represents the decreasing weight of the reservoir as garnet crystallizes. Equation (12) is a rearranged

form of Eq. (4). Introducing Eqs. (11) and (12) into Eq. (10) and rearranging, we obtain the following expression for the extended fractionation model incorporating an exchange equilibrium term:

$$1-\frac{W^G}{W^0}=\left[\frac{M_G(a+K_D-1)-K_D}{(K_D(1-M_G)+M_G)(M_0-1)}\right]^{\frac{1-K_D-a}{K_D-a}} \cdot\left[\frac{aM_G}{K_DM_0+M_GM_0(1-K_D)}\right]^{\frac{a}{K_D-a}} \tag{13}$$

or finally

$$f(M_G)=\left[\frac{M_G(a+K_D-1)-K_D}{(K_D(1-M_G)+M_G)(M_0-1)}\right]^{\frac{1-K_D-a}{K_D-a}} \cdot\left[\frac{aM_G}{K_DM_0+M_GM_0(1-K_D)}\right]^{\frac{a}{K_D-a}}+\frac{W^G}{W^0}-1=0. \tag{14}$$

Equation (14) is a function of only the weight fraction of the cation in the garnet edge, once a value is given for the extent of crystallization term, W^G/W^0. This latter term can be evaluated knowing that W^G is proportional to the cube of the garnet radius. W^0 is incorporated into the curve fitting parameter, A:

$$\frac{W^G}{W^0}=\mathrm{A}r^3 \tag{15}$$

where

$$A\equiv\frac{4\pi\rho_g}{3W^0}. \tag{16}$$

r is the radius and ρ_g is the density of the garnet crystal. Hollister (1969) evaluated the initial weight of the system, W^0, by using the sum of the estimated weights of the ferromagnesian minerals involved in the growth of the particular garnet. Similarly, Atherton (1968) incorporated his curve fitting term as the effective size of the mineral reservoir from which *one* garnet is crystallizing as suggested by a modal analysis of the minerals in the rock thin section.

A Newton-Raphson iterative technique is used to determine the root, M_G, of Eq. (14). Therefore, given values of the constants K_D, M_0, a and A, along with the radius of the garnet, we can determine the weight fraction of the component at the edge of the garnet. This process is repeated for each radius position to produce the complete zoning profile.

Figure 1 compares the simple Rayleigh fractionation model (Eq. 1) and the nonlinear exchange equilibrium model (Eq. 14) to the measured manganese profile in a garnet analyzed by Hollister (1966). Figure 1 states the values used for K_D, M_0, a and A. We have improved the fit of the Hollister fractionation model by decreasing the A parameter in the simple theory; and this value is used to obtain the nonlinear exchange model. There is *no* major difference between the MnO zoning curves as produced by either model. The use of the more correct exchange equilibrium term alters the theoretical profile by only 0.08 wt.% MnO at the maximum difference near the radial position of 200 μm.

The effect of varying the parameter a in the K_D expression (Eq. 4) at constant λ was analyzed. Normally, this term is set equal to unity to represent the simple two cation exchange process. However, the value of a has been reduced to values as low as 0.25 (with appropriate changes in K_D, so that $K_D = a\lambda$) to yield a fractionation profile (MnO core concentration is approximately 7 wt.%) with deviations no greater than 0.02 wt.% from the profile obtained with a equal to one and the same value of λ. Similar behavior occurs for greater Mn core compositions. For example, if the core MnO composition is 47 wt.%, the deviations between the profiles are not more than 0.04 wt.% whether $a=1$ or $a=0.25$ at constant λ values. Clearly, the a term is not a major influential parameter in the exchange equilibrium fractionation model except to relate K_D and λ.

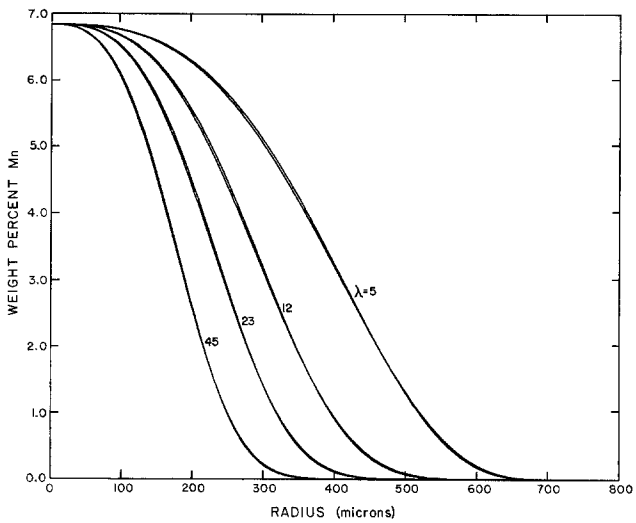

Fig. 2. Comparison between the simple Rayleigh and exchange equilibrium ($a=1$) isothermal fractionation profiles for a minor component with various values of λ and the corresponding K_D: $\lambda=45$, $K_D=48.2$; $\lambda=23$, $K_D=24.6$; $\lambda=12$, $K_D=12.8$; $\lambda=5$, $K_D=5.3$. $A=2624\,\mathrm{cm}^{-3}$ for all curves. Although barely observable the exchange profile is the upper curve at high concentrations then crosses the simple Rayleigh profile to become the lower curve near the 2 weight percent position

The small difference between the two theoretical curves suggests that Hollister's model is appropriate in describing the MnO zoning of the British Columbian garnets and that MnO partitioning is adequately described by a trace element partitioning term (Eq. 2). Figure 2 exhibits the theoretical profiles generated by both models for four different fractionation factor values. Excellent agreement occurs between each case.

Application of the same models for a major component, however, results in greater disagreements. Figure 3 shows the profiles for a zoned component initially at 47 wt.%. Here the exchange equilibrium model disagrees with the simple partition model by concentration differences of up to 4 wt.%. The difference between the two models increases as the fractionation factor or distribution coefficient decreases. For fractionation factors less than unity, concave upward profiles would be produced. In this case, the disagreement between the models decreases as the fractionation or distribution term decreases. It is apparent that the exchange equilibrium fractionation model is more appropriate than the Hollister partition model in describing the chemical zoning of major components (>10 wt.%). The compositional dependency of the partition fractionation factor of a component is dealt with successfully by the incorporation of a constant but nonlinear exchange equilibrium coefficient.

It is interesting to note that as the weight fraction terms, M_G and M_0, approach trace element proportions, the exchange equilibrium model (Eq. 13) reduces to the simple par-

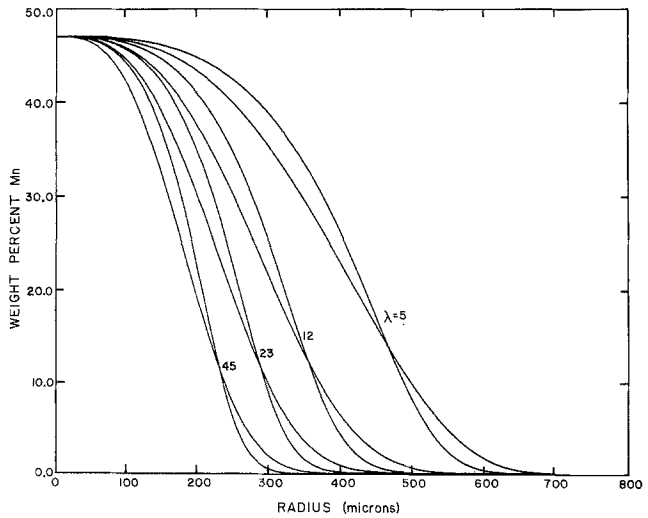

Fig. 3. Comparison between the simple Rayleigh and exchange equilibrium ($a=1$) isothermal fractionation profiles for a major component with various values of λ and the corresponding K_D: $\lambda=45$, $K_D=84.0$; $\lambda=23$, $K_D=42.5$; $\lambda=12$, $K_D=21.7$; $\lambda=5$, $K_D=8.5$. $A=2624\,\mathrm{cm}^{-3}$ for all curves. The exchange profile is the upper curve at high concentrations then crosses the simple Rayleigh profile to become the lower curve near the 13 weight percent position

tition fractionation model. Thus, if M_G and M_0 are much less than unity and $K_D=a\lambda$, as demonstrated earlier, the first factor of the right hand side of Eq. (13) reduces to unity, leaving:

$$1-\frac{W^G}{W^0}=\left[\frac{aM_G}{a\lambda M_0+M_G M_0(1-a\lambda)}\right]^{\frac{1}{\lambda-1}}. \tag{17}$$

The second term of the denominator is negligible because it involves the product of two numbers much smaller than one. Upon rearranging, we obtain an expression identical to the usual fractionation model:

$$M_G=\lambda M_0\left(1-\frac{W^G}{W^0}\right)^{\lambda-1}. \tag{18}$$

The exchange equilibrium fractionation model can be very useful in describing the major element zoning profiles of metamorphic garnets. It can also be applied to magma crystallization processes for monitoring major element distributions in phenocrysts and in the magma. This application would extend the work of Neuman et al. (1954), McIntire (1963) and Albarede and Bottinga (1972) who used the linear partition fractionation model for observing trace element distributions in the crystallizing magma.

Temperature and Growth Dependent Fractionation Model

The previous section indicates that use of λ rather than K_D is correct for minor cations (e.g., <10 wt. %). However, there are other additional important corrections to the simple Rayleigh fractionation model. The normal zoning pattern of manganese in garnet, decreasing from core to rim, is usually explained by the simple Rayleigh model. This model fails, though, when attempting to describe an increase of MnO towards the rim, as found in some metamorphic environments (Birk 1973; Kretz 1973). A fractionation factor less than unity would be required to produce the latter MnO profile using the isothermal Rayleigh model. This is highly unlikely since the large Mn^{2+} cation has a preferential affinity toward the cubic site of garnet relative to the octahedral sites of the matrix minerals. This was observed by Hollister (1969) who determined the initial MnO fractionation factors, λ_0, as ranging from 22 to 42 for metapelitic garnets. Therefore, the wide variety of MnO zoning profiles underscores the important influence of the growth process as well as temperature changes upon the fractionation process.

Recent papers have qualitatively explained the observed chemical zoning by allowing for temperature changes during the crystal growth (Tracy et al. 1976; Thompson et al. 1977). Increasing temperature during a prograde growth event would alter the distribution term and therefore change the equilibrium concentration of the cation being fractionated into the garnet edge. Similarly, a decrease in temperature would alter the distribution term but in the opposite direction and produce the reverse zoning profile. (It is assumed that cation diffusion will be ineffective in maintaining a homogeneous garnet.) The chemical composition of garnets from metamorphic terranes would probably reflect effects of both temperature changes and the depletion of the matrix minerals during crystal growth.

The role of time during growth is handled *implicitly* in the derivation of the isothermal fractionation model by use of the *extent of crystallization* term. However, if temperature also changes with time, we must treat the time dependence of the growth in a more explicit manner. To proceed, therefore, the initial differential equation (Eq. 5) is divided by the time interval, dt:

$$\frac{dW_m^R}{dt}=M_G\frac{dW_R}{dt}. \tag{19}$$

Dividing both sides of Eq. (19) by W_m^R and using Eqs. (2) and (8), we obtain:

$$\frac{1}{W_m^R}\frac{dW_m^R}{dt}=\frac{\lambda(t)}{W_R(t)}\frac{dW_R}{dt}. \tag{20}$$

The same notation as used earlier is continued here. Note that the weight of the reservoir, $W_R(t)$, and the fractionation factor, $\lambda(t)$, must now be given as functions of time. Integrating the left hand side of Eq. (20), we obtain the general form of the solution to our new time dependent model:

$$\ln W_m^R=\ln W_m^{R^0}+\int_0^t\frac{\lambda(t)}{W_R(t)}\left(\frac{dW_R}{dt}\right)dt. \tag{21}$$

$W_m^{R^0}$ represents the initial weight of the cation in the reservoir minerals.

The temperature dependent fractionation factor, $\lambda(T)$ (a precursor of $\lambda(t)$), will be treated as a linear partition term. We have already shown in the previous section that this usage, which is certainly valid for trace element concentrations, can also be used to satisfactorily monitor minor components (approximately 10 wt. % or less). The temperature dependence of the partition term is given by the standard thermodynamic formula:

$$\lambda(T)=\lambda_\infty\exp\left(-\frac{\Delta H^0}{RT}\right) \tag{22}$$

where λ_∞ is the pre-exponential term and ΔH^0 is the standard molar enthalpy of the cation exchange between the reservoir mineral and the garnet. ΔH^0 is generally a function of pressure and temperature as well as of the composition of the considered phases. Within certain ranges of these three parameters, however, ΔH^0 can be considered as a constant during the growth process. Equation (22) can be rewritten as:

$$\lambda(T)=\lambda_0 \exp\left[-\frac{\Delta H^0}{R}\left(\frac{\Delta T}{T T_0}\right)\right] \tag{23}$$

where λ_0 represents the value of the fractionation term at some initial temperature T_0. ΔT is defined as T_0-T. The temperature history is introduced by assuming a linear variation of temperature with time:

$$T=T_0-st. \tag{24}$$

s, as used here, represents a cooling (retrograde) rate if positive or a heating (prograde) rate if negative. If ΔT is small relative to T_0, T is approximated by T_0 and Eq. (23) therefore reduces to:

$$\lambda(t)=\lambda_0 \exp(-\alpha t) \tag{25}$$

where

$$\alpha \equiv \frac{\Delta H^0 s}{R T_0^2}. \tag{26}$$

The time dependence of W_R is obtained by considering the growth rate of garnet crystallizing from the reservoir:

$$\frac{dW^G}{dt}=-\frac{dW_R}{dt}=4\pi r^2 \rho_g \frac{dr}{dt} \tag{27}$$

where r is the radius of the garnet at time t and ρ_g is the garnet density. Equation (27) follows from the conservation of mass during the conversion of reservoir material into garnet. For the present case, let us assume a constant growth velocity, v, for the garnet. This condition is relaxed in a later section of this paper. We can generalize our solution and the earlier isothermal models by allowing for several stages of garnet growth as during successive metamorphic events. The radius of the garnet would then be given by:

$$r=r_0+vt \tag{28}$$

where r_0 represents the initial radius of the garnet at the onset of the growth event. Combining Eqs. (27) and (28) we obtain:

$$-\frac{dW_R}{dt}=4\pi(r_0+vt)^2 \rho_g v. \tag{29}$$

$W_R(t)$ is obtained by integrating the previous expression:

$$W_R(t)=W^0-\tfrac{4}{3}\pi\rho_g((r_0+vt)^3-r_0^3) \tag{30}$$

where W^0 is the initial weight of the reservoir.

Substituting Eqs. (25), (29) and (30) into Eq. (21) we obtain:

$$\ln W_m^R=\ln W_m^{R^0}-\int_0^t \frac{(\lambda_0 \exp(-\alpha t))(4\pi(r_0+vt)^2 \rho_g v)}{(W^0-\frac{4}{3}\pi(r_0+vt)^3 \rho_g+\frac{4}{3}\pi r_0^3 \rho_g)}\,dt. \tag{31}$$

This expression can be integrated numerically, or analytically once the exponential term is expanded. Appendix B provides details of the analytical evaluation of the integral.

To obtain the cation content at the garnet edge, Eqs. (2) and (8) are combined to give:

$$M_G(t)=\lambda(t)\frac{W_m^R(t)}{W_R(t)} \tag{32}$$

or

$$M_G(t)=\lambda_0 \exp(-\alpha t)\frac{W_m^R(t)}{W_R(t)} \tag{33}$$

where the reservoir weight terms are given by Eqs. (30) and (31).

Equation (33) is an exact solution to the problem of partitioning cations from a homogeneous mineral reservoir into the edge of a growing garnet in the presence of a linear change in temperature. We have generalized this solution to account for any precrystallized garnet and for either a heating or cooling event. However, the crystal growth rate has been constrained to be constant. The required input parameters for evaluating Eq. (33) include those given below:

M_G^0, initial weight fraction of cation in garnet
M_0, initial weight fraction of cation in reservoir
λ_0, initial fractionation factor, M_G^0/M_0
ΔH^0, enthalpy change for fractionation process
s, heating or cooling rate for growth event
T_0, initial temperature of system
v, radial growth rate of garnet
r_0, initial radius of garnet
W^0, initial weight of reservoir required for growth of any one garnet
$W_m^{R^0}$, initial weight of cation in reservoir, $M_0 W^0$.

Garnet chemical zoning profiles generated during growth can be modeled by Eqs. (30), (31) and (33). The corresponding radial position will be given by Eq. (28) for each time increment. The application of this general model to garnets grown during a retrograde event is presented in the next section.

Application of Temperature and Growth Dependent Model

In this section we apply the growth model derived in the previous section to the garnets of the Phillipston area of Massachusetts. The rock units of this area were subjected to high grade regional metamorphism during the Acadian orogeny with peak conditions at 675 °C and 5.0 kbar (Thompson 1974). A summary of the metamorphic terrane of the area and the locality of the particular outcrop (well past the second sillimanite isograd is provided by Fig. 1 of Lasaga et al. (1977).

The high grade rock contains large crystals of almandine-pyrope garnet. The major matrix minerals include biotite, cordierite, plagioclase, quartz, sillimanite and graphite. The garnets themselves are filled with randomly distributed inclusions of quartz, ilmenite and to a lesser extent biotite. These garnets possess a dodecahedral (roughly spherical) crystal habit and range in size from less than 1 mm to almost 15 mm in diameter. We will be concerned with only the larger-sized garnets in the present application. Richardson (1982) provides a thorough analysis and discussion of the mineralogy and geochemistry of the particular outcrop.

An ETEC automated electron microprobe analyzer was

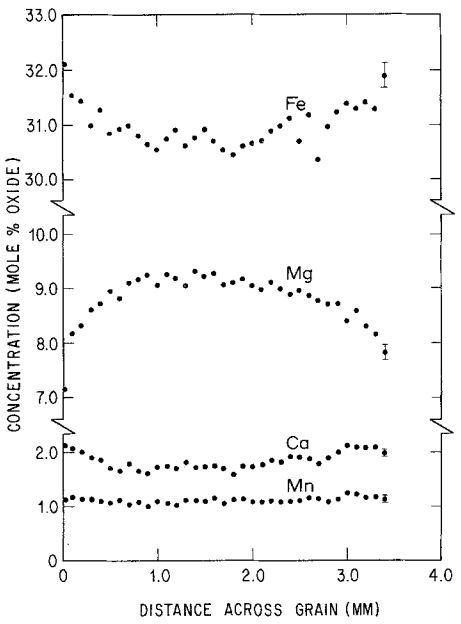

Fig. 4. Compositional profile across garnet A3 from Phillipston, Massachusetts. Analytical uncertainties are represented by the *brackets* on the right of the profile

used to obtain step scan analyses across selected garnets. Data reduction was performed using the correction scheme of Bence and Albee (1968) with the correction factors of Albee and Ray (1970). A typical zoning profile for the major cations is presented in Fig. 4. The iron and magnesium profiles complement each other across the grain; iron increases while magnesium decreases from the core region to the outer rim. Calcium and manganese, which are present in much smaller concentrations, exhibit only slight zoning behavior at the edge of the garnet. Silicon, aluminium and titanium remain unzoned in all of the garnets analyzed. The zoning patterns exhibited by the large garnets are spherically symmetrical as determined by several profile scans across each grain and appear to be uninfluenced by the immediately adjacent matrix minerals. As a good approximation, the zoning profiles can be considered within the binary system of the iron and magnesium end members. The mirror image profiles of these two cations are the result of maintaining charge balance in the eight-coordinated site of the garnet crystal lattice. The small fluctuations exhibited by iron and magnesium in their profiles probably represent analytical error or, in some cases, local exchange and diffusion effects between the garnet and a nearby inclusion. In addition, the microprobe electron beam produces an excitation volume which may encounter these inclusions to produce modified garnet analyses.

Lasaga et al. (1977) determined that the smaller and more numerous Phillipston garnets, those with diameters less than 1 mm, developed their zoning properties during a retrograde exchange and diffusion of iron and magnesium with the neighboring ferromagnesian minerals. These zoning profiles are similar in pattern to those of the larger garnets but are restricted to only the outer 30 μm of the garnet and *only* when in contact with cordierite or biotite. Similar iron and magnesium zoning behavior has also been noted in other high grade almandine garnets (Gable and Sims 1969; Grant and Weiblen 1971; Hess 1971; Tracy et al. 1976). All of these studies hypothesized the development of this zoning during a high temperature retrograde cation exchange process.

The major portion of the literature reporting garnet zoning describes both magnesium and iron as increasing from center to rim. Manganese antithetically decreases from the center producing a bell-shaped profile (Harte and Henley 1966; Hollister 1966; Atherton and Edmunds 1966, Linthout and Westra 1968). This normal zoning behavior is common to the low and medium grade pelitic rocks and probably represents a primary formation without interference by chemical diffusion. The high grade Phillipston garnets, on the other hand, will be more apt to homogenize by chemical diffusion and produce an unzoned crystal with a concomitant lowering of the manganese concentration. This latter point has been supported by the observed decrease of garnet manganese content with increasing metamorphic grade (Miyashiro 1953; Müller and Schneider 1971).

The effect of a temperature change during garnet crystallization must be considered in an analysis of the zoning profiles of the large Phillipston garnets. The iron-magnesium exchange distribution term (K_D) between garnet and a reacting phase (cordierite or biotite) will be altered by any temperature trends and will naturally be dependent upon the actual continuous reaction (see Thompson 1976). If chemical diffusion is ineffective in the garnet, cation zoning profiles will develop during growth. Cygan (1980) determined a definite trend in Fe−Mg K_D's (between core and rim of garnet and the neighboring ferromagnesian phase) which indicated a retrograde growth process for the large garnets. Similarly, Grant and Weiblen (1971) relied upon a decrease in temperature but suggested *resorption* of garnet to produce their zoning profiles, which are similar to those of this study. They proposed a continuous reaction involving the equilibrium assemblage garnet + biotite + cordierite + anthophyllite ± hypersthene. The cations were redistributed from the resorbed edge of the garnet uniformly throughout the rest of the garnet volume. Presumably, they attributed this redistribution to chemical diffusion. We believe that these distances (up to 40 % of the initial radius) are usually much too large to allow simple lattice diffusion to keep up with resorption, as required by their model. It therefore seems that resorption is an improbable mechanism for generating the desired profiles. These data imply that the large Phillipston garnets *grew* during a *retrograde* event so as to produce a magnesium profile decreasing from core to rim as iron increases.

A reexamination of the large garnet zoning profiles (see Fig. 4) suggests the existence of an essentially homogeneous core region surrounded by an outer region comprised of steep concentration gradients in magnesium and iron. Cygan and Lasaga (1979) suggested initial garnet growth during the prograde metamorphic event followed by homogenization of the garnets by volume diffusion at the peak temperature. During the cooling event several of the garnets continued to grow and developed the outer region of zoning characteristic of the larger garnets. The smaller grains were probably prevented from further growth due to the lack of reacting materials or some other kinetic factor and therefore were only capable of cation exchange with neighboring minerals during the retrograde event. This hypothesized growth history satisfactorily predicts the chemical zoning behavior exhibited by both sizes of garnet from Phillipston.

The large garnets provide a good example for the application of the temperature and growth dependent fractionation model which was derived in the previous section. We will only be concerned with generating the theoretical magnesium concentration profile in the garnet for several reasons. The

mirror-like profile of iron is obtained from the magnesium profile as a result of charge balance in the binary substitution. Also, the microprobe analyzer has improved absolute precision in the analysis of smaller concentrations, in this case, the magnesium concentration. This is the result of the restrictions imposed by the counting statistics for each element and the individual standards used. Finally, the temperature dependent fractionation model assumes a linear fractionation factor which has already been shown for the isothermal case to deviate from the exact distribution fractionation solution at high concentrations of the cation. These deviations are kept to a desirable minimum by using the magnesium concentrations which are no greater than 6 wt. % MgO.

Several parameters must be specified for inclusion in the model. Lasaga et al. (1977) determined a minimum cooling rate, s, of 100 °C per million years for the Phillipston area. While the exact nature of the growth reaction is not clear at this point (see Richardson 1982), it is reasonable to estimate the enthalpy for the fractionation, ΔH^0, at 6.5 kcal/mole as taken from the exchange reaction evaluated by Lasaga et al. (1977). The initial cation concentration of the garnet was taken as the average value of the homogeneous core region and the initial radius, r_0, is denoted approximately by the sudden onset of zoning in the magnesium profile. The initial cation concentration of the reservoir was obtained by averaging the magnesium analyses of the neighboring homogeneous cordierite minerals. We are assuming in this application that the retrograde growth of garnet was at the expense of cordierite or some other similar ferromagnesian reservoir phase. The initial fractionation factor at $T_0 = 675$ °C is calculated using Eq. (2) assuming that the initial cation concentrations in the garnet and the reservoir minerals were preserved through geologic time and are given directly by the microprobe analyses. The simplifying assumption is that chemical diffusion was negligible throughout the retrograde growth process but yet was responsible for the homogenization at the peak metamorphic temperature (see below).

The garnet growth rate, v, is an unknown quantity. Crystal growth data for garnet, or for that matter any metamorphic mineral, is lacking in the geologic literature. An important study of metamorphic mineral growth rates is provided by Fisher (1977) in which the diffusion-controlled growth of andalusite-biotite segregations was examined. It is interesting to obtain an approximate value for a *minimum* growth rate by assuming a simple lattice diffusion-controlled growth for garnet. We are ignoring any possibly enhanced growth rates created by fluid infiltration or intergranular diffusion. Nielsen (1964) gives the following equation for the growth velocity of a spherical grain as limited by the transport of one component to the grain interface through a solution or mineral reservoir:

$$v = \frac{dr}{dt} = \frac{D\bar{V}(C_\infty - C_s)}{r} \tag{34}$$

where D is interpreted as the binary diffusion coefficient for the reservoir mineral, e.g., cordierite as given by Lasaga et al. (1977). $\bar{V}$ is the molar volume for the garnet. $(C_\infty - C_s)$ is the difference between the bulk concentration of the one component in the reservoir and the concentration of the component at the surface of the growing garnet. A value for C_s was obtained from the cordierite exchange data for the smaller Phillipston garnets (see Lasaga et al. 1977). Therefore, for the larger-sized garnet A3 from Phillipston, Eq. (34) gives a limiting velocity of 0.0024 cm/million year at 675 °C. For the case of garnet growth from biotite, the diffusion-controlled growth rate will be slightly higher based on the faster diffusion rates in this mineral. These diffusion-controlled growth rates are only crude limiting cases and should not be accepted as representative of the actual growth mechanism. Cordierite and biotite generally do not occur completely surrounding the Phillipston garnets, therefore limiting this possible mode of crystal growth. In fact, we show below that the model yields much higher growth rates suggesting another growth-limiting mechanism.

Having determined the initial values of the parameters s and r_0 to be used in the growth model for the Massachusetts garnets, the values of the standard enthalpy for magnesium exchange, ΔH^0, the initial weight of the reservoir, W^0, and the garnet growth rate, v, are obtained from the best fit to the observed profiles. A theoretical composition profile for magnesium in garnet A3 as generated by Eq. (33) is presented in Fig. 5 along with the observed data points. The calculation uses the values $W^0 = 0.20$ g, $v = 0.040$ cm/m.y. and $\Delta H^0 = 4.0$ kcal/mole. The growth occurs during cooling from 675 °C to 475 °C. The fit of the theoretical curve to the measured profile has been optimized by varying the W^0, v and ΔH^0 parameters. Their physical significance and their influence upon the theoretical zoning profile will be discussed later. Note that, if *all* W^0 were converted into garnet, a spherical crystal 5 mm in diameter would form. Although the present model does not provide an ideal fit to the observed data, the incorporation of a cooling rate in the model does yield a fractionation profile that is the *reverse* of the profile that would be generated by the isothermal Rayleigh model. This clearly shows the importance of considering the temperature change in any growth event.

The difference in curvature between the measured profile and the temperature dependent model is primarily due to the constant velocity assumption. Realistically for a drop in temperature from 675 °C to 475 °C, there will be a corresponding decrease in growth velocity. A decreasing velocity could possibly reverse the curvature and provide a better fit to the measured profile. We treat this time dependent velocity growth process in the last section of this paper.

None of the fractionation models presented in this paper allow for modification of the garnet by chemical diffusion. At high enough temperatures this process plays an important role in determining the extent of compositional zoning (Anderson and Buckley 1973, 1974; Anderson and Olympio 1977; Lasaga 1979; Lasaga et al. 1977). Any zoning patterns which may have initially existed in the Phillipston garnets were effectively smoothed out by diffusion at the peak metamorphic temperature of 675 °C. Certainly, the diffusion rates would still be effective during the early parts of the retrograde growth. This process is neglected in applying the temperature dependent fractionation model to the large-sized Phillipston garnets. However, it should be noted that the growth distances are typically 1,000 μm while the penetration distances due to exchange and diffusion alone are only on the order of 30 μm (see Lasaga et al. 1977). Thus, in the case of retrograde growth our assumption may be reasonable. A numerical model including the effects of diffusion, exchange and growth will be presented in a forthcoming paper.

A growth rate of 0.040 cm/m.y. was required in Fig. 5 to approximate the measured garnet profile. This velocity, considerably greater than the rate suggested by the diffusion-

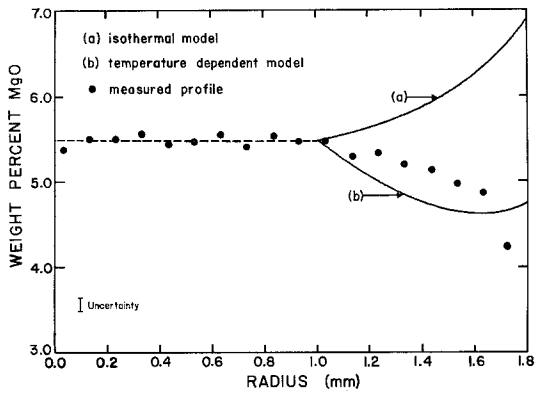

Fig. 5. Theoretical zoning profile for MgO in garnet A3: (*a*) isothermal fractionation model with $\lambda=0.58$; (*b*) temperature and growth dependent model with $\lambda_0=0.58$, $v=0.040$ cm/million year and $\Delta H^0=4.0$ kcal/mole. $W^0=0.20$ g for both curves. The *dots* represent the measured profile of MgO in weight percent

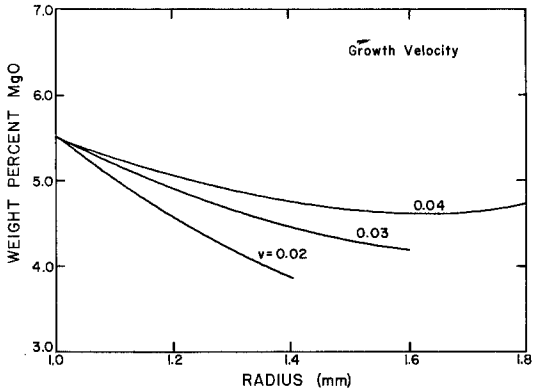

Fig. 7. The influence of the crystal growth velocity, v, upon the temperature and growth dependent fractionation model profile of garnet A3; $\lambda_0=0.58$, $\Delta H^0=4.0$ kcal/mole and $W^0=0.20$ g. v values are in units of cm/million year

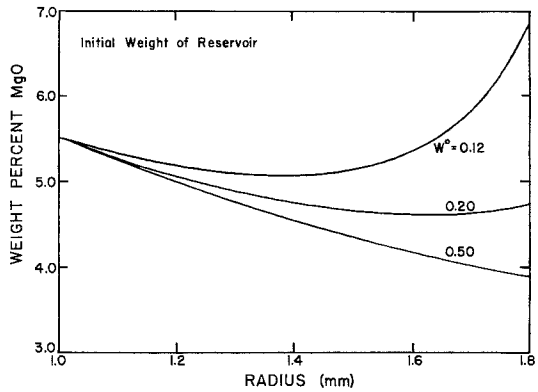

Fig. 6. The influence of the initial weight of the mineral reservoir, W^0, upon the temperature and growth dependent fractionation model profile of garnet A3; $\lambda_0=0.58$, $v=0.040$ cm/million year and $\Delta H^0=4.0$ kcal/mole. W^0 values are in units of g

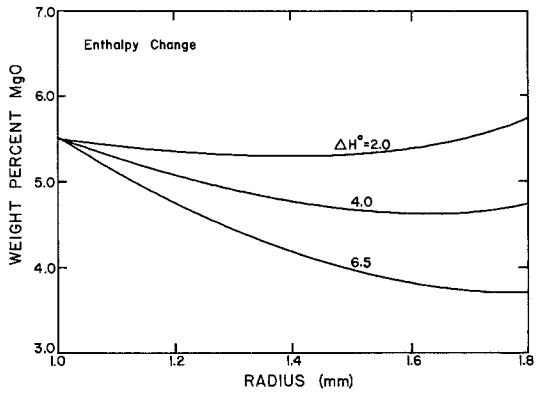

Fig. 8. The influence of the enthalpy change of cation partitioning, ΔH^0, upon the temperature and growth dependent fractionation model profile of garnet A3; $\lambda_0=0.58$, $v=0.040$ cm/million year and $W^0=0.20$ g. ΔH^0 values are in units of kcal/mole

controlled growth mechanism, is capable of producing the desired volume of new garnet for an allowed growth period of 2 m.y. Reasonable approximations of the other large Phillipston garnet profiles were produced utilizing the same growth rate. The greater velocity required stresses the importance of intergranular transport in the reservoir. Utilization of grain boundary diffusion coefficients (see Fisher 1978) in Eq. (34) provides similar order-of-magnitude values for the growth rate as that determined from the temperature dependent fractionation model. The best fit growth rate can eventually be linked to the actual rate of the garnet-producing reaction and may be representative of the rates of numerous metamorphic growth processes. Certainly, such kinetic data are important to the petrologist in understanding the generation of metamorphic terranes.

It is very important to analyze the effect of varying the major parameters involved in the temperature dependent model. The initial weight of the reservoir, W^0, limits the extent of zoning produced during the garnet growth. Figure 6 demonstrates the decrease in zoning produced by increasing the amount of material available in the reservoir. This result is reasonable considering the lesser extent of crystallization allowed for the same crystallization time. Figures 7 and 8 show the zoning relationships for similar changes in the growth velocity and fractionation enthalpy, respectively, for crystal growth during the temperature drop from 675 °C to 475 °C. Initial retrograde growth is not necessarily restricted to the peak temperature at 675 °C and may have started later in the cooling event at lower temperatures. The effect of increasing the growth velocity will be to increase the extent of the chemical zoning in the garnet in addition to the obvious result of producing larger crystals. This effect is accountable by the greater rate of incorporation of a cation into a growing garnet for a given crystallization time, thereby depleting the reservoir faster to produce the greater amount of zoning.

Finally in Fig. 9, we demonstrate a special case where the depletion of the reservoir during the fractionation process gradually overrides the temperature effect. The growth rate is fast enough relative to the cooling rate so that the mineral reservoir is quickly depleted of material causing the profile to reverse itself towards higher concentrations and approach the isothermal Rayleigh model curve. This process demonstrates a possible mechanism which under appropriate conditions can generate a reversal in the zoning pattern.

The temperature dependent fractionation growth model is completely general and can be applied equally well to prograde and retrograde growth events. This model does reduce to the simple isothermal Rayleigh model with the incorporation of a zero temperature change rate. In this capacity, the model allows for the complete monitoring of crystal growth

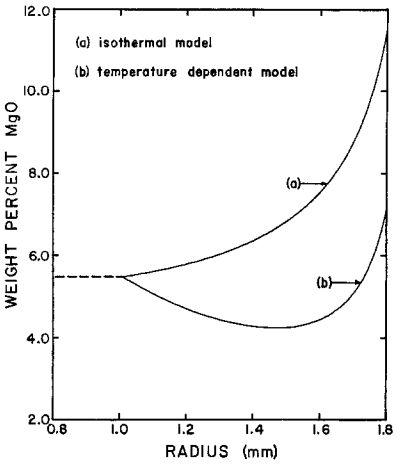

Fig. 9. Special case of temperature and growth dependent fractionation model demonstrating the possible generation of MgO chemical profile which reverses its zoning behavior; $T_0=675\,^{\circ}C$, $s=100^{\circ}$/million year, $\lambda_0=0.58$, $v=0.020$ cm/million year, $\Delta H^0=4.0$ kcal/mole and $W^0=0.010$ g. Crystal growth was allowed to proceed for 4 million years

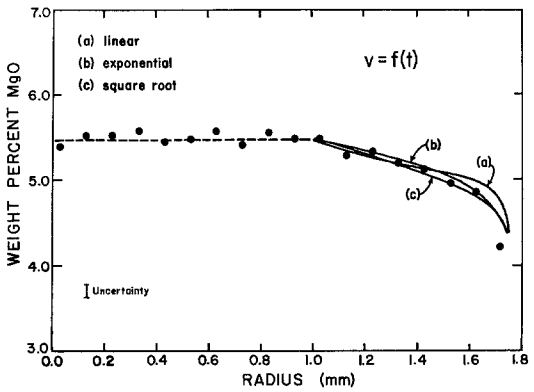

Fig. 10. Theoretical zoning profiles for MgO in garnet A3 based upon a temperature dependent fractionation model incorporating a time dependent growth velocity term — numerical solutions: (*a*) linear growth rate decay, $v_0=0.070$ cm/million year, $k=0.033$ cm/million year^2; (*b*) exponential growth rate decay, $v_0=0.090$ cm/million year, $k=1.10$ million year^{-1}; (*c*) square root-*t* growth rate decay, $v_0=0.090$ cm/million year, $k=0.057$ cm/million year$^{3/2}$. $\Delta H^0=4.0$ kcal/mole and $W^0=0.20$ g for all curves. The *dots* represent the measured profile of MgO in weight percent

with time as dictated by a given growth rate. In addition, the temperature dependent model is not restricted to the continued growth of preexisting crystals. The model satisfactorily generates the zoning of a complete crystal by assuming an infinitestimal initial radius (i.e., $r_0=0$) in the calculations.

Time Dependent Velocity Model

In natural systems we expect the growth rate to vary as a function of temperature and therefore of time. For example, a 200 °C temperature drop could possibly decrease the velocity term to such an extent so as to prevent any appreciable garnet growth in the Phillipston garnets. Therefore, we should incorporate this variation in the growth rate. In particular, a decreasing growth rate could reverse the curvature of the constant velocity chemical profile presented in Fig. 5. Any increased agreement between the theoretical and measured profiles would provide further evidence in support of the retrograde growth theory for the large Phillipston garnets.

To study the effects of varying growth rates, three growth rate-time relationships are introduced into the fractionation model: linear, exponential and square root behavior:

$$v(t)=v_0-kt, \tag{35}$$

$$v(t)=v_0\exp(-kt), \tag{36}$$

$$v(t)=v_0-kt^{1/2}. \tag{37}$$

v_0 is the initial growth velocity at temperature T_0 and k is an undetermined constant which is related to the rate of change of velocity during the growth process. The forms chosen in Eqs. (35)–(37) are based on the expressions used for v in various types of crystal growth theories (see Nielsen 1964; Jackson 1967). Corresponding to Eqs. (35)–(37) are three radius-time expressions:

$$r(t)=r_0+v_0t-\tfrac{1}{2}kt^2, \tag{38}$$

$$r(t)=r_0+\frac{v_0}{k}-\frac{v_0}{k}\exp(-kt), \tag{39}$$

$$r(t)=r_0+v_0t-\tfrac{2}{3}kt^{3/2}. \tag{40}$$

Equations (35)–(37) are each separately introduced into Eq. (27) (for dr/dt) which represents the change in reservoir weight with time for the temperature and growth dependent fractionation model. The resulting expression is integrated to obtain the expression for the weight of the reservoir analogous to Eq. (30). The new reservoir weight expressions are then inserted into Eq. (21). A preliminary investigation avoided the direct solution to the now complex integral of Eq. (21) by the use of a numerical integration scheme. The calculation of the cation content in the garnet edge is then obtained using the same procedure described in the constant velocity model.

Figure 10 presents the profiles obtained for the three numerically evaluated models. The square root-*t* velocity model provides the best fit to the measured profile, but this result cannot be taken as proof of a diffusion-controlled growth process. Such simple growth velocity behavior may be useful in modelling crystal growth but its use must be cautioned for completely describing the complex nature expected of natural garnet growth.

The exponential growth velocity numerical model is capable of providing an additional source of kinetic data. The growth rate, described by Eq. (36), is an exponential function of time and should be representative of a thermally activated process. It is possible to extract activation energy values for the growth rate from the exponent. An activation energy of 20 kcal/mole is obtained employing the k value determined from the best fit of the model profile. Values of this energy may provide some additional help in understanding the mechanism of metamorphic crystal growth.

It will be beneficial to investigate the square root-*t* velocity model in detail in view of the best fit to the measured data. To derive the exact solution to this model, we require the analytical integration of the time term in the W_m^R expression:

$$\ln W_m^R=\ln W_m^{R^0}+\int_0^t\frac{(\lambda_0\exp(-\alpha t))}{W_R(t)}\left(\frac{dW_R}{dt}\right)dt \tag{41}$$

where

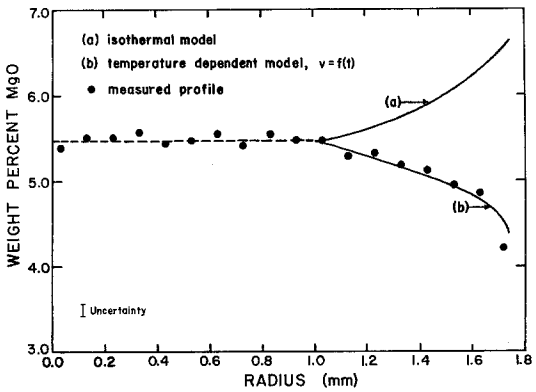

Fig. 11. Theoretical zoning profile for MgO in garnet A3: (*a*) temperature dependent fractionation model incorporating a time dependent growth velocity term – analytical solution; $\lambda=0.58$, $v_0=0.090$ cm/million year, $k=0.057$ cm/million year$^{3/2}$ and $\Delta H^0=4.0$ kcal/mole. $W^0=0.20$ g for both curves. The *dots* represent the measured profile of MgO in weight percent

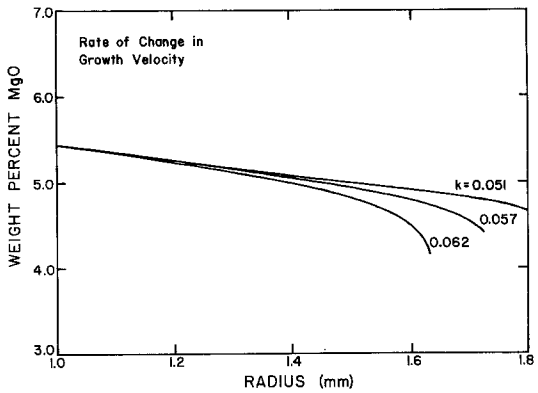

Fig. 12. The influence of the growth velocity change rate, k, upon the temperature dependent fractionation model incorporating a square root-t dependent growth velocity term; $\lambda_0=0.58$, $v_0=0.090$ cm/million year, $\Delta H^0=4.0$ kcal/mole and $W^0=0.20$ g. k values are in units of cm/million year$^{3/2}$

$$-\frac{dW_R}{dt}=4\pi(r_0+v_0t-\tfrac{2}{3}kt^{3/2})^2\,\rho_g(v_0-kt^{1/2}) \tag{42}$$

and

$$W_R(t)=W^0-ar_0^2v_0t-ar_0v_0^2t^2-a(\tfrac{4}{9}r_0k^2+\tfrac{1}{3}v_0^3)t^3 -\tfrac{4}{9}ak^2v_0t^4+\tfrac{2}{3}ar_0^2kt^{3/2}+\tfrac{4}{3}ar_0kv_0t^{5/2} +\tfrac{2}{3}av_0^2kt^{7/2}+\tfrac{8}{81}ak^3t^{9/2} \tag{43}$$

and where now

$$a\equiv 4\pi\rho_g. \tag{44}$$

The analytical evaluation of the integral in Eq. (41) can be done in a similar fashion, although more complex, as the evaluation of the integral in Appendix B. Finally, the cation concentration in the garnet edge, M_G, is obtained by the use of Eq. (33) but now using the reservoir weight relations given by Eq. (43) and the integrated form of Eq. (41).

The resulting profile for magnesium is presented in Fig. 11 along with the corresponding isothermal model. The initial growth rate, v_0, incorporated in this application is similar to the rate used in the earlier constant velocity model. The value of the k term was initially chosen arbitrarily and then altered appropriately to determine its effect upon the zoning profile. The final k value incorporated in the model provides the optimum fit to the measured profile of garnet A3. The equation for the growth rate is now:

$$v(t)=0.090-0.057t^{1/2}\ \text{(cm/m.y.)}. \tag{45}$$

Hence, in the time it takes to cool through 200 °C (2 m.y.), v changes from 0.090 cm/m.y. to 0.009 cm/m.y. Figure 12 presents an analysis of changing the values of k in this model and its effect upon the generated chemical profiles.

An important conclusion to be made from these results is that the incorporation of varying growth rates into the model can significantly improve the modeling of zoning profiles. The values obtained for v_0 and k in our calculations are optimized to yield the best fit. The generality of these values for metapelitic or metavolcanic assemblages must await further application of our model to other garnet localities.

Conclusion

We have developed several extensions to the simple isothermal fractionation growth model. These additions provide the refinements required in applying crystal growth theory to natural minerals. The complicated growth history of certain minerals, primarily the metamorphic garnets, can now be properly deduced from the exhibited chemical zoning profiles.

We have found the assumption of a linear fractionation term adequate in describing the profile of certain major components. Limitations on this assumption can be determined by consideration of the analytical uncertainties and their relationship to the disagreements between the simple partition and exchange equilibrium isothermal models as shown in Figs. 2 and 3.

The temperature and growth dependent fractionation model provides a sound basis for quantitatively examining compositional profiles of minerals. This general model enables one to monitor several stages of crystal growth as dictated by the system size, bulk composition, temperature range, growth rate and cooling or heating rate. The importance of considering the temperature change during a fractionation growth process was demonstrated by the reverse profile obtained in applying the model. The internal balance between temperature change and fractionation and their effect on the growth process is determined by the selected parameters. The extent of crystallization term, W^G/W^0, can be instituted for monitoring the depletion state of the reservoir and the compositional gradient created in the garnet. The incorporation of a time dependent growth rate greatly refines the fractionation model and provides a good foundation for its application in complex geological environments.

The application of the theory is not limited to growth of metamorphic garnets. Fractionation growth processes can be modeled in numerous geological instances, including additional igneous and metamorphic refractory minerals, crystallization of magmas, isotope distributions and geothermometry. The use of these fractionation growth models, or geospeedometers, will lead to the eventual understanding of the complex disequilibrium processes found in geological systems.

Acknowledgements. This study represents part of R.T. Cygan's M.S. thesis at The Pennsylvania State University. Comments by J.G. Blencoe, E.K. Graham and D.M. Kerrick on an early draft of the paper were of extreme help. George W. Fisher and an anonymous reviewer provided valuable critiques of the manuscript which greatly improved the final version. This work was supported in part by NSF Grant EAR 78-01785 to A.C. Lasaga and by a NSF Energy-Related Traineeship and a Mining and Mineral and Mineral Fuel Conservation Fellowship to R.T. Cygan.

Appendix A. Solution of isothermal exchange equilibrium fractionation model differential equation

To obtain the solution of the exchange equilibrium model differential equation (Eq. 9), an integrating factor is required. Let:

$$M_R = \frac{W_m^R}{W_R}. \tag{A1}$$

Actually, this expression is equivalent to the weight fraction of the cation in the reservoir as given previously by Eq. (8). Taking the derivative of this quotient we obtain:

$$d\left(\frac{W_m^R}{W_R}\right) = -\left(\frac{W_m^R}{W_R}\right)\frac{dW_R}{W_R} + \frac{dW_m^R}{W_R} = dM_R \tag{A2}$$

which upon rearranging produces:

$$\frac{dW_m^R}{dW_R} = \left(\frac{W_m^R}{W_R}\right) + W_R\frac{dM_R}{dW_R}. \tag{A3}$$

Inserting Eq. (A3) into Eq. (9) and rearranging to separate variables we obtain Eq. (A4) where the reservoir weight terms have been replaced by M_R:

$$\frac{dW_R}{W_R} = \frac{M_R(1-K_D)-a}{M_R(K_D-a)(M_R-1)}dM_R \tag{A4}$$

or

$$\frac{dW_R}{W_R} = \frac{1-K_D}{(K_D-a)(M_R-1)}dM_R - \frac{a}{M_R(K_D-a)(M_R-1)}dM_R. \tag{A5}$$

The last term of this equation can be written in terms of simple partial fractions, which produces an easily integrated equation:

$$\int_{W^0}^{W_R}\frac{dW_R}{W_R} = \frac{1-K_D}{K_D-a}\int_{M_0}^{M_R}\frac{1}{M_R-1}dM_R - \frac{a}{K_D-a}\int_{M_0}^{M_R}\frac{1}{M_R-1}dM_R + \frac{a}{K_D-a}\int_{M_0}^{M_R}\frac{1}{M_R}dM_R \tag{A6}$$

or

$$\ln\left(\frac{W_R}{W^0}\right) = \frac{1-K_D}{K_D-a}\ln\left(\frac{M_R-1}{M_0-1}\right) - \frac{a}{K_D-a}\ln\left(\frac{M_R-1}{M_0-1}\right) + \frac{a}{K_D-a}\ln\left(\frac{M_R}{M_0}\right). \tag{A7}$$

After rearranging Eq. (A7) and then exponentiating both sides of the resulting equation, we obtain the final form of the solution to Eq. (9) as given below:

$$\frac{W_R}{W^0} = \left(\frac{M_R-1}{M_0-1}\right)^{\frac{1-K_D-a}{K_D-a}}\left(\frac{M_R}{M_0}\right)^{\frac{a}{K_D-a}}. \tag{A8}$$

Appendix B. Evaluation of integral for temperature dependent fractionation model

With the assumption of changing temperature during garnet growth, as given by Eq. (24), we have introduced several complicated functions of temperature and, hence, time. The limiting mathematical maneuver required in the temperature dependent fractionation model is the evaluation of the integral in Eq. (31). The integrand can be rewritten as:

$$\mathrm{INT} \equiv av\int_0^t \frac{(\lambda_0\exp(-\alpha t))(r_0+vt)^2}{\left(W^0 - \frac{a}{3}(r_0+vt)^3 + \frac{a}{3}r_0^3\right)}dt \tag{B1}$$

where

$$a \equiv 4\pi\rho_g. \tag{B2}$$

It is desirable to alter the form of the exponential term, $\lambda(t)$, to a polynomial in order to simplify the integration. Expanding Eq. (25) as a quadratic in t, we obtain:

$$\lambda(t) = \lambda_0 - \beta t + \gamma t^2 \tag{B3}$$

where

$$\beta \equiv \lambda_0\alpha \tag{B4}$$

and

$$\gamma \equiv \tfrac{1}{2}\lambda_0\alpha^2. \tag{B5}$$

This approximation is very good for applications, including those of this study, where the absolute value of αt is less than one. Introducing the new form of $\lambda(t)$ in place of the exponential term in Eq. (B1) we obtain:

$$\mathrm{INT} = av\int_0^t \frac{(\lambda_0-\beta t+\gamma t^2)(r_0+vt)^2}{\left(W^0 - \frac{a}{3}(r_0+vt)^3 + \frac{a}{3}r_0^3\right)}dt. \tag{B6}$$

Expanding both numerator and denominator polynomials, we obtain:

$$\mathrm{INT} = av\int_0^t \frac{v^2\gamma t^4 + (2r_0v\gamma - \beta v^2)t^3 + (\lambda_0 v^2 + \gamma r_0^2 - 2\beta r_0 v)t^2 + (2r_0 v\lambda_0 - \beta r_0^2)t + r_0^2\lambda_0}{-\frac{a}{3}v^3t^3 - ar_0v^2t^2 - ar_0^2vt + W^0}dt. \tag{B7}$$

Synthetic division of the improper polynomial fraction reduces the integrand to:

$$\mathrm{INT} = av\int_0^t\left[-\frac{3\gamma}{av}t + \frac{3r_0\gamma + 3\beta v}{av^2} + \frac{At^2+Bt+C}{\left(-\frac{a}{3}v^3t^3 - ar_0v^2t^2 - ar_0^2vt + W^0\right)}\right]dt \tag{B8}$$

where

$$A \equiv r_0^2\gamma + \lambda_0 v^2 + r_0\beta v, \tag{B9}$$

$$B \equiv 2r_0^2\beta + 2r_0v\lambda_0 + \frac{3r_0^3\gamma}{v} + \frac{3\gamma W^0}{av}, \tag{B10}$$

$$C \equiv r_0^2\lambda_0 - \frac{3r_0\gamma W^0}{av^2} - \frac{3\beta W^0}{av}. \tag{B11}$$

The first two terms of Eq. (B8) are easily integrated whereas the third term requires reduction to partial fractions before integrating. This third term, defined as $L(t)$, can be rewritten with its denominator factored, giving:

$$L(t) \equiv \frac{At^2+Bt+C}{(t-k)(lt^2+mt+n)} \tag{B12}$$

where

$$k \equiv \frac{1}{v}\left(r_0^3 + \frac{3}{a}W^0\right)^{1/3} - \frac{r_0}{v}, \tag{B13}$$

$$l \equiv -\frac{av^3}{3}, \tag{B14}$$

$$m \equiv -ar_0 v^2 - \frac{kav^3}{3}, \tag{B15}$$

$$n \equiv -\frac{W^0}{k}. \tag{B16}$$

Using partial fractions to reduce Eq. (B12) we obtain:

$$L(t) = \frac{Dt+E}{lt^2+mt+n} + \frac{F}{t-k} \tag{B17}$$

where

$$D \equiv \frac{\frac{mA}{l} + \frac{nA}{kl} - \frac{C}{k} - B}{\frac{m}{l} + \frac{n}{kl} + k}, \tag{B18}$$

$$E \equiv \frac{1}{kl}(nA - nD - Cl), \tag{B19}$$

$$F \equiv \frac{1}{l}(A - D). \tag{B20}$$

The first term of Eq. (B17) can be integrated by means of a simple substitution. Combining the result with all of the integrated forms of the simple terms from Eqs. (B8) and (B17), we obtain the final form of the integrated Eq. (B1):

$$\begin{aligned} \mathrm{INT} = &-\tfrac{3}{2}\gamma t^2 + \left(\frac{3r_0\gamma}{v} + 3\beta\right)t + avF\ln\left(1 - \frac{t}{k}\right) \\ &+ \frac{av}{l\sqrt{G}}\left(E - \frac{Dm}{2l}\right)\left[\tan^{-1}\left(\frac{t+\frac{m}{2l}}{\sqrt{G}}\right) - \tan^{-1}\left(\frac{m}{2l\sqrt{G}}\right)\right] \\ &+ \frac{avD}{2l}\ln\left[\frac{\left(t+\frac{m}{2l}\right)^2 + G}{\left(\frac{m}{2l}\right)^2 + G}\right] \end{aligned} \tag{B21}$$

where

$$G \equiv \frac{n}{l} - \frac{m^2}{4l^2}. \tag{B22}$$

References

Albarede F, Bottinga Y (1972) Kinetic disequilibrium in trace element partitioning between phenocryst and host lava. Geochim Cosmochim Acta 36:141–156

Albee AL, Ray L (1970) Correction factors for electron-probe microanalysis of silicates, oxides, carbonates, phosphates and sulfates. Anal Chem 42:1408–1414

Anderson DE, Buckley GR (1973) Zoning in garnets – diffusion models. Contrib Mineral Petrol 40:87–104

Anderson DE, Buckley GR (1974) Modeling of diffusion controlled properties of silicates. In: Hofmann AW et al (eds) Geochemical transport and kinetics. Carnegie Inst Washington Publ, pp 31–52

Anderson DE, Olimpio JC (1977) Progressive homogenization of metamorphic garnets, South Morar, Scotland: evidence for volume diffusion. Can Mineral 15:205–216

Atherton MP (1968) The variation in garnet, biotite and chlorite composition in medium grade pelitic rocks from the Dalradian, Scotland, with particular reference to the zonation in garnet. Contrib Mineral Petrol 18:347–371

Atherton MP (1976) Crystal growth models in metamorphic tectonites. Philos Trans R Soc London Ser A283:255–270

Atherton MP, Edmunds WM (1966) An electron microprobe study of some zoned garnets from metamorphic rocks. Earth Planet Sci Lett 1:185–193

Bence AE, Albee AL (1968) Empirical correction factors for the electron microanalysis of silicates and oxides. J Geol 76:382–403

Birk D (1973) Chemical zoning in garnets of the Kashabowie group, Shebandowan, Ontario. Can Mineral 12:124–128

Blackburn WH (1969) Zoned and unzoned garnets from the Grenville gneisses around Gananoque, Ontario. Can Mineral 9:691–698

Brown EH (1969) Some zoned garnets from the greenschist facies. Am Mineral 54:1662–1677

Cygan RT (1980) Crystal growth and the formation of chemical zoning in natural garnets. Pennsylvania State University MS thesis, 194 pp

Cygan RT, Lasaga AC (1979) Formation of chemically zoned garnets by diffusion and crystal growth. EOS 60:741

de Béthune P, Laduron D, Bacquet J (1975) Diffusion processes in resorbed garnets. Contrib Mineral Petrol 50:197–204

Emiliani F, Venturelli G (1972) Sharp compositional zoning in an almandine garnet. Can Mineral 11:464–472

Finlay CA, Kerr A (1979) Garnet growth in a metapelite from the Moinian rocks of Northern Sutherland, Scotland. Contrib Mineral Petrol 76:185–191

Fisher GW (1977) Nonequilibrium thermodynamics in metamorphism. In: Fraser DG (ed) Thermodynamics in geology. Reidel, Dordrecht, pp 381–403

Fisher GW (1978) Rate laws in metamorphism. Geochim Cosmochim Acta 42:1035–1050

Gable DJ, Sims PK (1969) Geology and regional metamorphism of some high grade cordierite gneisses, Front Range, Colorado. Geol Soc Am Spec Pap 128:1–87

Grant JA, Weiblen PW (1971) Retrograde zoning in garnet near the second sillimanite isograd. Am J Sci 270:281–296

Harte B, Henley KJ (1966) Occurrence of compositionally zoned almanditic garnets in regionally metamorphosed rocks. Nature 210:689–692

Hess PC (1971) Prograde and retrograde equilibria in garnet-cordierite gneisses in south-central Massachusetts. Contrib Mineral Petrol 30:177–195

Hollister LS (1966) Garnet zoning: an investigation based on the Rayleigh fractionation model. Science 154:1647–1651

Hollister LS (1969) Contact metamorphism in the Kwoiek area of British Columbia: an end member of the metamorphic process. Geol Soc Am Bull 80:2465–2494

Jackson KA (1967) Current concepts in crystal growth from the melt. In: Reiss H (ed) Progress in solid state chemistry, vol 4. Pergamon Press, New York, pp 53–80

Kretz R (1973) Kinetics of the crystallization of garnet at two localities near Yellowknife. Can Mineral 12:1–20

Lasaga AC (1979) Multicomponent exchange and diffusion in silicates. Geochim Cosmochim Acta 43:455–469

Lasaga AC, Richardson SM, Holland HD (1977) The mathematics of cation diffusion and exchange between silicate minerals during retrograde metamorphism. In: Saxena SK, Bhattacharji S (eds) Energetics of geological processes. Springer, New York, pp 353–388

Linthout K, Westra L (1968) Compositional zoning in almandine-rich garnets and its relation to the metamorphic history of their host rocks. Proc K Ned Akad Wet Ser B 71:297–312

Loomis TP (1975) Reaction zoning of garnet. Contrib Mineral Petrol 52:285–305

McIntire WL (1963) Trace element partition coefficients – a review of theory and application to geology. Geochim Cosmochim Acta 27:1209–1264

Miyashiro A (1953) Calcium-poor garnet in relation to metamorphism. Geochim Cosmochim Acta 4:179–208

Miyashiro A, Shido F (1973) Progressive compositional change of garnet in metapelite. Lithos 6:13–20

Müller G, Schneider A (1971) Chemistry and genesis of garnets in metamorphic rocks. Geochim Cosmochim Acta 31:178–200

Neumann H, Mead J, Vitaliano CJ (1954) Trace element variation

during fractional crystallization as calculated from the distribution law. Geochim Cosmochim Acta 6:90–99

Nielsen AE (1964) Kinetics of precipitation. Pergamon Press, New York, 151 pp

Rayleigh L (1902) On the distillation of binary mixtures. Philos Mag 4:521–537

Richardson SM (1982) The assemblage garnet + cordierite + biotite + sillimanite in a metavolcanic rock at Phillipston, Massachusetts. Contrib Mineral Petrol (in press)

Thompson AB (1974) Calculation of muscovite-paragonite-alkali feldspar phase relations. Contrib Mineral Petrol 44:173–194

Thompson AB (1976) Mineral reactions in pelitic rocks: I. prediction of P–T–X(Fe–Mg) phase relations. Am J Sci 276:401–424

Thompson AB, Tracy RJ, Lyttle PT, Thompson JB (1977) Prograde reaction histories deduced from compositional zonation and mineral inclusions in garnet from the Gassetts schist, Vermont. Am J Sci 277:1152–1167

Thompson JB, Norton SA (1968) Paleozoic regional metamorphism in New England and adjacent areas. In: Zen E et al (eds) Studies of Appalachian geology, Northern and Maritime. Wiley, New York, pp 319–328

Tracy RJ, Robinson P, Thompson AB (1976) Garnet composition and zoning in the determination of temperature and pressure of metamorphism, central Massachusetts. Am Mineral 61:762–775

Woodsworth GJ (1977) Homogenization of zoned garnets from schists. Can Mineral 15:230–242

Yardley BWD (1977) An empirical study of diffusion in garnet. Am Mineral 62:793–800

Received September 8, 1980;
Accepted in revised form February 3, 1982